Inorganica Chimica Acta 566 (2024) 122022

Contents lists available at ScienceDirect

Inorganica Chimica Acta

journal homepage: www.elsevier.com/locate/ica

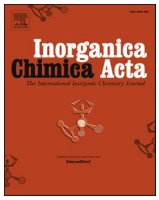

Synthesis, structural and computational study, DNA binding and cytotoxic activity of Cu(II) complexes of 6- and 7-chloro-2-oxo-1,2-dihydroquinoline-3-carbaldehyde-2-furoyl-hydrazones

Thangavel Thirunavukkarasu [a], Hazel A. Sparkes [b], Valentina Gandin [c], Cristina Marzano [c], Roberta Bertani [a,d,j], Mirto Mozzon [a], Anna Scettri [a], Alberto Albinati [e,f], Francesco Demartin [g], Girolamo Casella [h,i], Francesco Ferrante [i], Alfonso Zoleo [k], Paolo Sgarbossa [a,j,*], Karuppannan Natarajan [l,*]

[a] Department of Industrial Engineering, University of Padova, Via F.Marzolo 9, Padova 35131, Italy
[b] School of Chemistry, University of Bristol, Cantock's Close, Bristol BS8 1TS, UK
[c] Department of Pharmaceutical and Pharmacological Sciences, University of Padova, Via F.Marzolo 5, 35131, Italy
[d] CNR-ICMATE, Corso Stati Uniti 4, 35127 Padova, Italy
[e] CNR-ICCOM, Via Madonna del Piano, 50119 Sesto Fiorentino, Italy
[f] University of Milano, Milan, Italy
[g] UNITECH COSPECT, Università degli Studi di Milano, via Golgi 19, 20133 Milano, Italy
[h] Dipartimento di Scienze della Terra e del Mare (DiSTeM), Università degli Studi di Palermo, Via Archirafi, 22, 90123 Palermo, Italy
[i] Dipartimento di Fisica e Chimica "Emilio Segrè", Università degli Studi di Palermo, Viale delle Scienze, 90128 Palermo, Italy
[j] CIRCC, Consorzio Interuniversitario per le Reattività Chimiche e la Catalisi, Bari, Italy
[k] Dipartimento di Scienze Chimiche, Università degli Studi di Padova, Via F. Marzolo 1, 35131 Padova, Italy
[l] Research and DevelopmentCenter, PSGR Krishnammal College for Women, Coimbatore 641004. India

A R T I C L E I N F O

Dedicated to Giovanni Natile, dear friend and mentor, on the occasion of his eightieth birthday.

Keywords:
Cu(II) hydrazone complexes
X-ray-structures
EPR data
DFT
Cytotoxicity tests

A B S T R A C T

Three new coordination complexes of Cu(II) ions made from two hydrazone ligands, 7-chloro-2-oxo-1,2-dihydroquinoline-3-carbaldehyde-2-furoyl-hydrazone (HL1) and 6-chloro-2-oxo-1,2-dihydroquinoline-3-carbaldehyde-2-furoyl-hydrazone (HL2) have been synthesized and fully characterized by spectroscopic techniques. Their crystal and molecular structures revealed distorted square pyramidal mononuclear complexes: $[(L1)Cu(H_2O)_2](NO_3)\cdot 3H_2O$, **1**$(NO_3)$, $[(L2)Cu(H_2O)_2](NO_3)\cdot 2H_2O\cdot CH_3OH$, **2**$(NO_3)$, and $[(L2)Cu(NO_3)(CH_3OH)]\cdot 2CH_3OH$, **3**, comprising the ligand (L1 and L2) in tridentate fashion (ONO) with two water molecules in $\mathbf{1}^+$ and $\mathbf{2}^+$, and a single methanol molecule and a nitrate ion in **3** in their respective copper coordination spheres. EPR spectra in frozen methanol revealed the occurrence of several species arising from different coordination environments. A detailed DFT investigation on the energetics of solvents exchange (H_2O, MeOH, and DMSO) and simulation of the EPR parameters showed that the exchange processes occur easily in solution. The value g_z indicated the occurrence of a dimeric aggregate for $\mathbf{2}^+$. The new copper complexes exhibited a noticeable antiproliferative activity with IC_{50} values in the micromolar range against HCT-15, H157, BxPC3, PNS-1, and A431 cell lines and they were found to be 3-fold more effective than cisplatin against pancreatic PSN-1 cell lines. Cross-resistance tests on A2780 and LoVo cancer cell lines and the corresponding multidrug or oxaliplatin resistant sublines showed that complexes **1**(NO_3) and **2**(NO_3) were equally cytotoxic to sensitive and resistant cells, thus overcoming multidrug and oxaliplatin resistance.

1. Introduction

Ever since the discovery of cisplatin for the treatment of cancer, there has been a continuous interest in the synthesis of other platinum complexes due to the fact that cisplatin and related compounds exhibited significant side effects such as nephrotoxicity, emetogenesis,

* Corresponding authors at: Department of Industrial Engineering, University of Padova, Via F.Marzolo 9, Padova 35131, Italy (P. Sgarbossa).
E-mail addresses: paolo.sgarbossa@unipd.it (P. Sgarbossa), knatraj66@gmail.com (K. Natarajan).

https://doi.org/10.1016/j.ica.2024.122022
Received 20 January 2024; Received in revised form 14 March 2024; Accepted 14 March 2024
Available online 15 March 2024

neurotoxicity and the emergence of resistance [1–10]. As a result, attention was focused on to design metal complexes which are less toxic, target-specific and with less resistance. It is well known that metal complexes exert the anticancer properties through their binding to DNA and inhibiting the growth of the tumor cells and hence, the design of small complexes that can bind and react at specific sequences of DNA has become essential. While DNA is considered the primary target for platinum-based drugs, other metal complexes have been subjected to multiple targets, such as proteins and other cell components [11]. The use of bio-essential metal centers in the rational design of anticancer drugs is considered an opportunity that could help facing both the selectivity and the resistance problems. Among the many bio-essential metals, copper is considered as a promising alternative to platinum since cisplatin itself was considered as most promising anticancer therapeutic due to the fact that it is able to use copper-transporting proteins to reach intracellular compartments [12–14]. In this area copper-based antineoplastic agents have been developed to act on the altered metabolism of cancer cells, which showed a differential response between the latter and normal cells [15–19]. Moreover, there have been few reports of copper complexes exhibiting an ability to hydrolytically cleave DNA [20–27]. In this respect, there has been continuous interest over the years in determining the mode and extent of binding of metal complexes to DNA and protein, as such information are important to understand the cleavage properties of metal complexes [22,23]. In this connection, copper complexes containing heterocyclic bases have been extensively explored by virtue of their strong interactions with DNA and cytotoxic activity [24–27]. So, by possessing the required biologically accessible redox potentials and high nucleobase affinity, they are potential reagents for further studies on DNA cleavage [21,22]. Furthermore, their interactions at the protein binding level also significantly affect their apparent distribution volume and elimination rate. Therefore, their interactions with serum albumins is important and has been central in the many studies of antitumoral metal-pharmaceutical pharmacokinetics and structure–activity relationships [10].

In addition to the metal ions present in the complexes, the ligands bound to the metal centre also have some influence in determining the possible interactions between the drug and the biological environment. Since the ligands bound to the metal centres are strategic in defining the possible interactions between the drug and the biological environment, a wide range of ligands have been tried with copper and among them, most notable ones are hydrazones [X-C(Z) = N-NH-C(=O)-Y], which can have a great variety of functional groups available, thus modulating structural, chemical, physical and coordination properties [28,29]. In this connection, many hydrazones and their copper complexes have provoked immense interest in their diverse biological and pharmaceutical activities such as anticancer and antioxidative activities [30–54].

Though a lot of hydrazones have been tried, those derived from dihydroquinoline and furan moieties, which themselves show potential biological activities, have not been well explored. This has aroused our interest in the synthesis of new ligands, namely, 7- and 6-chloro-2-oxo-1,2-dihydroquinoline-3-carbaldehyde derivatives bearing a furan moiety, and prepared the corresponding Cu(II) complexes. A very promising cytotoxic activity has been demonstrated by the new complexes against several human cancer cell lines derived from solid tumors, some of which are platinum-resistant or displaying multidrug resistance (MDR).

2. Experimental

2.1. General

All starting precursors were of analytical grade. 6-chloro-2-oxo-1,2-dihydroquinoline-3-carbaldehydes and 7-chloro-2-oxo-1,2-dihydroquinoline-3-carbaldehydes were prepared according to literature procedures [46,49]. CT-DNA was obtained from Sigma Aldrich and used as received. Elemental analyses (C, H, N) were performed on Vario EL III Elemental analyzer instrument. Melting points were determined with a Lab India instrument. The infrared spectra were obtained on a Perkin-Elmer Spectrum 100 FT IR spectrophotometer (KBr disks) in the range 4000–400 cm^{-1}. The electronic spectra of the complexes were recorded with a Perkin Elmer Lambda 25 spectrophotometer using DMSO as the solvent. ^{1}H and ^{13}C NMR spectra were obtained at 298 K on a Bruker Avance Neo 600 NMR operating at 600.13 and 150.9 MHz, respectively; δ values (ppm) are relative to Me_4Si for ^{1}H and ^{13}C. Suitable integral values for the proton spectra were obtained with a pre-scan delay of 10 s. The assignments of the proton resonances were performed by standard homonuclear chemical shift correlations (COSY, NOESY, TOCSY). The ^{13}C resonances were attributed through 2D-heterocorrelated COSY experiments: heteronuclear multiple quantum correlation (HMQC) with bilinear rotation decoupling [55] and quadrature along F1 have been achieved using the time proportional phase increment method for the hydrogen-bonded carbon atoms, heteronuclear multiple bond correlation (HMBC) [56,57] for the quaternary ones. EPR measurements were carried out by preparing 10^{-3} M solutions of the complexes in methanol. The EPR spectra have been collected in X band in frozen matrix (powder spectra) at 140 K, setting 0.5 mT modulation amplitude, sweep 200 mT, power 20 mW by using an EPR Bruker ECS106, equipped with TMH9019 cavity. ESI-MS analyses were performed using a Finningan LCQ-Duo ion-trap instrument, operating in positive ion mode (sheath gas flow N_2 30 au, source voltage 4.0 kV, capillary voltage 21 V, capillary temperature 200 °C). The He pressure inside the trap was kept constant. The pressure, directly read by an ion gauge (in the absence of the N_2 stream), was 1.33×10^{-5} Torr. Sample solutions were prepared by dissolving the compounds (3 mg) in DMSO (5 mL) and diluting 1 mL of the solution in CH_3CN (5 mL) immediately before analysis.

2.2. Synthesis of the ligands and copper(II) complexes

7-Chloro-2-oxo-1,2-dihydroquinoline-3-carbaldehyde hydrazone (HL1)

2-Furoic hydrazide (0.126 g, 1 mmol) dissolved in warm methanol (20 mL) was added to a methanol solution (20 mL) containing 0.207 g (1 mmol) of 7-chloro-2-oxo-1,2-dihydroquinoline-3-carbaldehyde. The mixture was refluxed for 5 h, during which a yellow precipitate was formed. The reaction mixture was then cooled to room temperature, and the yellow solid compound was filtered off, washed with methanol and dried under vacuum. Yield: 0.324 g (88.5 %). Mp: 317–318 °C, Elemental Anal. Calcd. for $C_{15}H_{10}N_3O_3Cl{\cdot}MeOH{\cdot}H_2O$ (MW 365.77): C, 52.54; H, 4.41; N, 11.49; Cl, 9.69. Found (%): C, 51.84; H, 4.14; N, 11.53; Cl 9.60. IR (KBr disks, cm^{-1}): 3450 (ms,br) ν_{NH+OH}; 1664 (s,br) $\nu_{C=O+C=N}$; 1597 (s) $\nu_{C=C}$; 1560 (m); 1188 (s); 1298 (m); 1017 (s); 961 (s); 772 (s). UV–visible (H_2O; λ_{max}, nm; ε, cm^{-1} M^{-1}): 348 (11798); 404 (17217). ^{1}H NMR (600 MHz, DMSO-d_6): δ = 8.47 (C3-H, 1H, s); 7.93 (C5-H, 1H, d, $^{3}J_{HH}$ 8.50 Hz); 7.27 (C6-H, 1H, dd, $^{3}J_{HH}$ 8.50 Hz, $^{4}J_{HH}$ 1.96 Hz); 7.36 (C8-H, 1H, d, $^{4}J_{HH}$ 1.96 Hz); 8.68 (C10-H, 1H, s); 7.34 (C13-H, 1H, d, $^{3}J_{HH}$ 3.58 Hz); 6.61 (C14-H, 1H, dd, $^{3}J_{HH}$ 3.58 Hz, $^{3}J_{HH}$ 3.44 Hz); 7.96 (C15-H, 1H, d, $^{3}J_{HH}$ 3.44 Hz); 12.10 (N1-H, 1H, s); 12.05 (N3-H, 1H, s). $^{13}C\{^{1}H\}$ NMR (600 MHz, DMSO-d_6): δ = 160.64 (C1 = O); 125.60 (C2); 134.12 (C3); 117.94 (C4); 130.71 (C5); 122.42 (C6); 135.62 (C7); 114.20 (C8); 138.54 (C9); 142.10 (C10); 154.10 (C11 = O); 146.10 (C12); 114.74 (C13); 111.90 (C14); 145.83 (C15). ESI (*m/z*, rel. ab.%, L1 = $C_{15}H_9N_3O_3Cl$, MM 314.70): $[L1 + Na]^+$, *m/z* 337 (90 %); $[2L1 + Na]^+$, *m/z* 652 (100 %); $[3\ L1 + Na]^+$, *m/z* 967 (25 %); $[4L1 + Na]^+$, *m/z* 1281 (20 %); $[5L1 + Na]^+$, *m/z* 1596 (20 %); $[6L1 + Na]^+$, *m/z* 1911 (5 %).

6-Chloro-2-oxo-1,2-dihydroquinoline-3-carbaldehyde hydrazone (HL2)

2-furoic hydrazide (0.126 g, 1 mmol) dissolved in warm methanol (20 mL) was added to a methanol solution (20 mL) containing 0.207 g (1 mmol) of 6-chloro-2-oxo-1,2-dihydroquinoline-3-carbaldehyde. The mixture was refluxed for 5 h, during which a yellow precipitate was formed. The reaction mixture was then cooled to room temperature, and the yellow solid compound was filtered off, washed with methanol and

dried under vacuum. Yield: 0.319 g (87.3 %). Mp: 314–316 °C, Elemental Anal. Calcd. for $C_{15}H_{10}N_3O_3Cl{\cdot}MeOH{\cdot}H_2O$ (MW 365.77): C, 52.54; H, 4.41; N, 11.49; Cl, 9.69. Found (%): C, 51.95; H, 4.26; N, 11.63; Cl, 9.58. IR (KBr disks, cm^{-1}): 3497 and 3407 (ms,br) ν_{NH+OH}; 1651 (s) $\nu_{C=O}$; 1598 (s) $\nu_{C=N+C=C}$; 1294(s); 1188 (s); 1008 (s); 858 (s); 773 (m). UV–visible (H_2O; λ_{max}, nm; ε, cm^{-1} M^{-1}): 255 (19771); 360 (12072). ^1H NMR (600 MHz, DMSO-d_6): δ = 8.46 (C3-H, 1H, s); 8.03 (C5-H, 1H, d, $^4J_{HH}$ 1.7 Hz); 7.57 (C7-H, 1H, dd, $^3J_{HH}$ 8.78 Hz, $^4J_{HH}$ 1.7 Hz); 7.35 (C8-H, 1H, d, $^3J_{HH}$ 8.78 Hz); 8.69 (C10-H, 1H, s); 7.34 (C13-H, 1H, d, $^3J_{HH}$ 3.50 Hz); 6.71 (C14-H, 1H, dd, $^3J_{HH}$ 3.50 Hz, $^3J_{HH}$ 3.28 Hz); 7.96 (C15-H, 1H, d, $^3J_{HH}$ 3.28 Hz); 12.16 (N1-H, 1H, s); 12.07 (N3-H, 1H, s). $^{13}C\{^1H\}$ NMR (600 MHz, DMSO-d_6): δ = 160.40 (C1 = O); 126.26 (C2); 133.82 (C3); 119.91 (C4); 127.73 (C5); 126.00 (C6); 130.82 (C7); 117.22 (C8); 137.46 (C9); 142.3 (C10); 154.60 (C11 = O); 146.00 (C12); 116.84 (C13); 111.90 (C14); 145.83 (C15). ESI (*m/z*, rel.ab.%, L2 = $C_{15}H_9N_3O_3Cl$, MM 314.70): $[L2 + Na]^+$, *m/z* 337 (100 %); $[2L2 + Na]^+$, *m/z* 652 (85 %); $[3L2 + Na]^+$, *m/z* 967 (30 %); $[4L2 + Na]^+$, *m/z* 1281 (15 %); $[5L2 + Na]^+$, *m/z* 1596 (25 %); $[6L2 + Na]^+$, *m/z* 1911 (15 %).

$[(L1)Cu(H_2O)_2](NO_3){\cdot}3H_2O$, 1($NO_3$)

$Cu(NO_3)_2{\cdot}3H_2O$ (0.5 mmol, 0.120 g) was taken in methanol (20 mL) and **HL1** (0.5 mmol, 0.155 g) was added to it. The mixture was continuously heated under reflux for 2 h. The resulting solution was allowed to cool. Slow evaporation of the solvent gave green crystals suitable for X-ray studies. They were filtered off, washed with cold methanol, and dried under vacuum. Yield, 0.226 g (85.2 %). Mp. 334–337 °C (dec). Elemental Anal. Calc. for $C_{15}H_{19}N_4O_{11}ClCu$ (MW 530.33): C, 33.97; H, 3.61; N, 10.56; Cl 6.68. Found (%): C, 33.71; H, 3.48; N, 10.28; Cl, 6.31. UV–visible (DMSO; λ_{max}, nm; ε, cm^{-1} M^{-1}): 435 (28820). IR (KBr disks, cm^{-1}): 3417 (ms, br) ν_{NH+OH}; 1634 (s,br) $\nu_{C=O+C=N+C=C}$; 1463 (s); 1290 (s); 1196 (s); 802 (s); 770 (s). ESI (*m/z*, rel.ab.%, $1^+ = C_{15}H_9N_3O_3ClCu$, MM 378): $[1 + H_2O]^+$, *m/z* 396 (25 %); $[1 + K]^+$, *m/z* 417 (100 %).

$[(L2)Cu(H_2O)_2](NO_3){\cdot}2H_2O{\cdot}CH_3OH$, 2($NO_3$)

$Cu(NO_3)_2{\cdot}3H_2O$ (0.5 mmol, 0.120 g) was taken in methanol (20 mL) and **HL2** (0.5 mmol, 0.155 g) was added to it. The mixture was continuously heated under reflux for 2 h. The resulting solution was allowed to cool. Slow evaporation of the solvent gave green crystals suitable for X-ray studies. They were filtered off, washed with cold methanol, and dried under vacuum.

Yield, 0.223 g (84.8 %). Mp. 330–332 °C (dec). Elemental Anal. Calc. for $C_{16}H_{21}N_4O_{11}ClCu$ (MW 544.36): C, 35.30; H, 3.89; N, 10.29; Cl, 6.51. Found (%): C, 35.72; H, 3.68; N, 10.13; Cl, 6.29. UV–visible (DMSO; λ_{max}, nm; ε, cm^{-1} M^{-1}): 434 (22978). IR (KBr disks, cm^{-1}): 3433 (ms,br) ν_{NH+OH}; 1646 (s) $\nu_{C=O}$; 1568 (s) $\nu_{C=N+C=C}$; 1461 (s), 1298 (s), 1194 (s); 771(s). ESI (*m/z*, rel.ab.%, $2^+ = C_{15}H_9N_3O_3ClCu^+$, MM 378): $[2 + H_2O]^+$, *m/z* 396 (35 %); $[2 + K]^+$, *m/z* 417 (100 %).

Upon dissolution of complex **2**(NO_3) in CH_2Cl_2 and slow evaporation in the presence of Et_2O, suitable crystals of $[(L2)Cu(NO_3)(CH_3OH)]{\cdot}2CH_3OH$, **3**, have been obtained.

2.3. X-ray crystallography

Data collection parameters (Tables S1, S9, S16), extended crystallographic data (Tables S2–S8, S10–S15, S17–S21), details of the solution and refinement of the structures and the crystallographic references are given in the Supplementary Information and in the cif files. Suitable crystals of **1**(NO_3) and **2**(NO_3) were obtained from methanol solutions (see Experimental §2.2) while those of $[(L2)Cu(NO_3)(CH_3OH)]{\cdot}2CH_3OH$, **3** have been obtained by redissolving the powder of **2**(NO_3) in CH_2Cl_2 and upon slow evaporation in presence of Et_2O. The low temperature data collections (T = 100 K) were carried out for **1**(NO_3) and **3** on a Rigaku XtaLAB Synergy diffractometer equipped with a HyPix Hybrid Pixel Array Detector (Cu $K_\alpha\lambda$ = 1.54184 Å), and for **2**(NO_3) on a Bruker APEX II diffractometer equipped with CCD detector (Mo $K_\alpha\lambda$ = 0.71073 Å). The structures were solved by direct methods (Superflip for **2**(NO_3) and ShelXT for **1**(NO_3) and **3**) and refined by full matrix least-squares using F^2 in ShelXL as implemented in WingX v 2021.3. All non-hydrogen atoms were refined anisotropically. The contribution of the hydrogen atoms in their calculated positions was included in the refinement using a riding model with isotropic displacement parameters (U(H) = 1.5 × U_{eq}(O), U(H) = 1.2 × U_{eq}(N)). The O—H protons, where possible, were located in the difference Fourier maps. The presence of hydrogens bonded to the N atoms was checked in the difference Fourier maps. Only the N1 atoms have bonded H atoms that were freely refined with isotropic displacement parameter.

2.4. Computational methods

Geometry optimizations were performed by using the Gaussian 16 package [58]. All the system models were treated at the DFT level by employing the B3LYP functional in conjunction with the third order Grimme's empirical correction for dispersion interactions, D3, [59] and the 6-311G(d,p) basis set. Calculations have been carried out both in vacuum and by considering methanol as bulk solvent by means of the SMD approach [60]. All the optimized structures were confirmed to be true minima by inspection of the harmonic frequencies (cartesian coordinates are given in Table S23). The same protocol has been used to calculate EPR parameters. Gibbs free energies have been used to discuss the coordination thermodynamics of water and methanol towards the metal centre.

2.5. DNA binding studies

The UV–VIS absorption spectroscopic studies and the DNA binding experiments were performed at room temperature. The purity of the CT-DNA in the buffer solution was verified by taking the ratio of the absorbance values at 260 and 280 nm, which was found to be 1.8:1, indicating that the DNA was sufficiently free of protein. The DNA concentration per nucleotide was determined by absorption spectroscopy using the molar extinction coefficient value of 6600 dm^3mol^{-1} cm^{-1} at 260 nm. The complexes were dissolved in a mixed solvent of 5 % DMSO and 95 % Tris-HCl buffer for all the experiments. Absorption titration experiments were performed with a fixed concentration of the compounds (25 μM) by gradually increasing the concentration of DNA (5–25 μM). While measuring the absorption spectra, an equal amount of DNA was added to both the test solution and the reference solution to eliminate the absorbance of DNA itself.

2.6. Experiments with human cancer cells

The compounds were dissolved in DMSO just before the experiment, and calculated amounts of drug solution were added to the cell growth media to a final solvent concentration of 0.5 %, which had no detectable effect on cell killing. Cisplatin was dissolved in 0.9 % NaCl solution. Cisplatin, oxaliplatin, and MTT (3-(4,5-dimethylthiazol-2-yl)-2,5-diphenyltetrazolium bromide) were obtained from Merck KGaA, Darmstadt, Germany.

2.7. Cell cultures

Human colon (LoVo and HCT-15), lung (H157) and pancreatic (BxPC3 and PSN-1) carcinoma cell lines were obtained from American Type Culture Collection (ATCC, Rockville, MD). The human ovarian cancer A2780 and its resistant subline, A2780 ADR, were kindly provided by Prof. Rigobello (Dept. of Biomedical Science of Padova University, Italy). Human cervical carcinoma cells A431 were kindly provided by Prof. F. Zunino (Division of Experimental Oncology B, Istituto Nazionale dei Tumori, Milan, Italy). LoVo-OXP cells were derived, using a standard protocol, by growing LoVo cells in increasing concentrations of oxaliplatin and following months of selection of resistant clones [61]. Cell lines were maintained in the logarithmic phase at 37 °C in a 5 % carbon dioxide atmosphere using the following

culture media containing 10 % fetal calf serum (Euroclone, Milan, Italy), antibiotics (50 units/mL penicillin and 50 μg/mL streptomycin) and 2 mM L-glutamine: RPMI-1640 medium (Euroclone) for HCT-15, H157, BxPC3, PSN-1, A431 cells; F-12 HAM'S (Sigma Chemical Co.) for LoVo, A2780ADR, and LoVo-OXP cells.

2.8. Cytotoxic activity

The growth inhibitory effect toward tumor cells was evaluated by means of the MTT assay. Briefly, (3–8) $\times 10^3$ cells/well, depending upon the growth characteristics of the cell line, were seeded in 96-well microplates in growth medium (100 μL). After 24 h, the medium was removed and replaced with fresh medium containing the compound to be studied at the appropriate concentration. Quadrupled cultures were established for each treatment. After 72 h, each well was treated with 10 μL of a 5 mg/mL MTT saline solution and, following 5 h of incubation, 100 μL of a sodium dodecyl sulfate (SDS) solution in 0.01 M HCl were added. After an overnight incubation, cell growth inhibition was detected by measuring the absorbance of each well at 570 nm using a Bio-Rad 680 microplate reader. The mean absorbance for each drug dose was expressed as a percentage of the control untreated well absorbance and plotted vs drug concentration. IC50 values, the drug concentrations that reduce the mean absorbance at 570 nm to 50 % of those in the untreated control wells, were calculated by the four-parameter logistic (4-PL) model. The evaluation was based on means from at least four independent experiments.

2.9. Statistical analysis

All the values are the means ± SD of not less than three measurements. Multiple comparisons were made by ANOVA followed by Tukey–Kramer multiple comparison test ($P < 0.05$), using GraphPad software.

3. Results and discussion

3.1. Synthesis and characterization

The synthetic route for the ligands and their corresponding copper complexes are shown in Scheme 1. The ligands **HL1** and **HL2** were synthesized by condensation of either 7-chloro- or 6-chloro-2-oxo-1,2-dihydroquinoline-3-carbaldehyde with 2-furoic hydrazide in methanol, respectively, as described in the Experimental section, and have been characterized by elemental analysis, ESI mass spectrometry, FTIR, UV–Vis, ^{1}H and ^{13}C NMR spectroscopic studies. A very small broad signal at 11.84 and 11.85 ppm in the ^{1}H NMR spectra in DMSO solution of **HL1** and **HL2**, respectively, can be attributed to the presence of an amide-iminol tautomerism (inset in Scheme 1), whose equilibrium will be shifted towards the iminol species upon copper coordination [62,63]. The NOESY spectra indicated the expected *E*-conformation of the ligands.

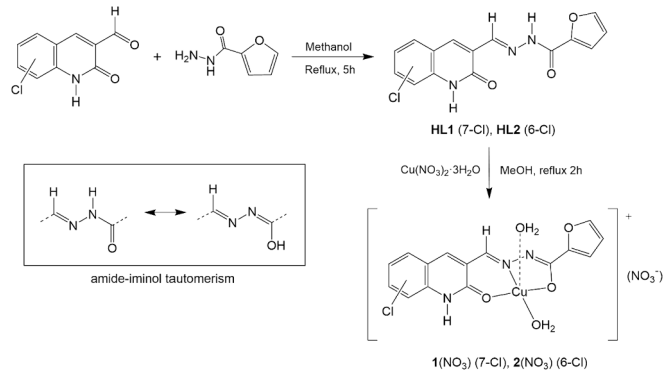

Scheme 1. The synthetic route for the ligands and of the corresponding Cu (II) complexes.

Cu(II) complexes were prepared by the reactions of the Schiff base ligands in methanol with $Cu(NO_3)_2{\cdot}3H_2O$ (1:1 M ratio) and obtained in good yields. They are air stable and soluble in ethanol, methanol, DMF, and DMSO. The compounds have been characterized by FTIR, UV–Vis spectroscopic studies and ESI-MS. The structures of all the copper complexes have been confirmed by single crystal X-ray diffraction studies. The decreasing of the $\nu_{(C=N)}$ and $\nu_{(C=O)}$ frequencies in the IR spectra of the Cu(II) complexes compared to that of the free ligands ($\Delta\nu_{(C=N+C=O)} = 30$ cm^{-1} for **1**(NO_3); $\Delta\nu_{(C=N+C=C)} = 30$ cm^{-1} and $\Delta\nu_{(C=O)} = 5$ cm^{-1} for **2**(NO_3)) clearly indicated the coordination of the ligands to the metal centre.

3.2. Crystal structures of the Cu(II) complexes

3.2.1. Solid state structure of 1(NO_3): [(L1)Cu(H_2O)$_2$][NO_3]·3H_2O

Fig. 1 shows an ORTEP view of the complex $\mathbf{1}^+$. A list of relevant bond lengths and angles is given in Table 1 together with the corresponding DFT calculated values for comparison. The N2, O2 and O3 atoms of the **L1** ligand and an oxygen-bound water molecules **(**Cu-O5 1.946 (2) Å) define the immediate coordination sphere of the Cu(II), showing a slightly distorted square planar geometry, with the Cu atom ca. 0.15 Å above the lsq-square plane defined by the Cu, O1, O2, N2 atoms (see Table S8). There is a weak interaction with a second H_2O molecule (at 2.217(2) Å) in apical position. Thus, the overall coordination geometry of the Cu centre is square pyramidal as often observed in related Cu complexes [46,49] bearing hydrazone ligands. Three more water molecules were found in the difference Fourier maps. The Cu-O and Cu-N bond distances fall in the expected range and are comparable with those in similar complexes reported in the literature [46,49]. The difference between the Cu-O1 and Cu-O2 separations may be explained by the different strain resulting from the formation of six and five atoms rings upon ligand-coordination to the Cu atom.

The agreement between the calculated and observed geometry is quite good as can be seen from the data in Table 1 and the overlay of the two structures shown in Fig. S7. The most significant differences between the observed and calculated distances are found in the Cu-O separations, and are easily explained by the different packing interactions. Upon coordination, the ligand is only slightly distorted with the planar dihydroquinoline and furan moieties making angles of ca. 3.1° and 6.2° respectively with the above defined lsq-plane. The molecular packing is dictated by a complex network of hydrogen-bonds between the oxygens of H_2O molecules (Figs. S5 and S6), the N atoms of the ligand and of the NO_3^- counterions (in the range 2.7–3.2 Å). Fairly weak π- π stacking interactions (at ca. 4.4 Å) between the planar quinoline and furan rings (see Figs. S4 and S6) are also present.

3.2.2. Solid state structure of 2(NO_3): [(L2)Cu(H_2O)$_2$][NO_3]·2H_2O·CH_3OH

The structure solution revealed, in the asymmetric unit, the presence of two crystallographically independent **2**(NO_3) units, four H_2O and two CH_3OH molecules. Both the $\mathbf{2}^+$ cations, the NO_3^- counterions, and the solvent molecules are related by two non-crystallographic inversion

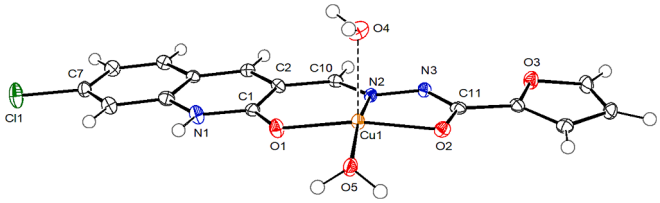

Fig. 1. Ortep view of the cation ($\mathbf{1}^+$) (ellipsoid drawn at 50 % probability).

Table 1
Selected Bond Lengths (Å) and Angles (deg) for Complex ($\mathbf{1}^+$) together with the corresponding DFT calculated values.

	X-ray	Methanol[a]	Vacuum[a]
Cu1-O1	1.947(2)	1.986	1.932
Cu1-O2	1.957(2)	1.971	1.913
Cu1-O4	2.217(2)	2.507	2.328
Cu1-O5	1.946(2)	2.033	2.038
Cu1-N2	1.954(2)	1.986	1.937
Cl1-C7	1.735(2)	1.757	1.738
O1-C1	1.265(3)	1.265	1.262
O2-C11	1.293(3)	1.298	1.302
N2-N3	1.385(3)	1.370	1.360
N2-C10	1.284(6)	1.297	1.296
N1-C1	1.351(3)	1.362	1.361
O1-Cu1-O2	165.28(7)	172.77	175.63
O1-Cu1-O4	97.48(7)	88.89	87.96
O2-Cu1-O4	95.77(7)	92.11	95.89
O1-Cu1-O5	90.19(7)	89.18	91.08
O2-Cu1-O5	93.88(7)	97.70	93.17
N2-Cu1-O5	167.53(8)	174.79	168.9
N2-Cu1-O4	92.24(7)	88.84	104.07
N3-N2-C10	117.4(2)	118.23	118.73
N2-N3-C11	109.6(2)	109.68	110.01

[a] Data calculated at B3LYP-GD3/6-311G(d,p) both in a vacuum and by considering the bulk solvent, methanol.

centers (pseudo inversion symmetry, see experimental and Fig. S8). The bond lengths and angles in the two independent **2**(NO_3) units (Mol A, Fig. 2, and B, respectively) are equal within 2σ (the only significant differences being in the Cu1-O4/Cu1a-O4a, Cu1-O5/Cu1a-O5a separations at 7σ and 5σ respectively). Thus, the values listed in Table 2 refer to one molecule only (A, Figs. S9 and S10) without averaging. The coordination around the Cu(II) centre may be described as a distorted square planar coordination as in **1**(NO_3) with the Cu atom 0.06 Å above and the O5 atoms 0.15 Å below the lsq-plane defined by the atoms Cu, O1, O2, N2 (see Table S15). There is a weak interaction with a second H_2O molecule (at 2.342(2) Å) in apical position leading to a square pyramidal coordination as in $\mathbf{1}^+$. The Cu-O and Cu-N bond distances fall in the expected range and are comparable with those in similar complexes reported in the literature [46,49] and to those found in **1**(NO_3). The only significant differences are those involving the Cu-OH_2 separations due to the different molecular packing interactions in the two complexes.

Upon coordination, the ligand is distorted only slightly with the planar dihydroquinoline and furan rings making angles of ca. 3.2° and 4.5°, respectively with the above defined mean coordination plane. The slightly different deformations of the ligand in $\mathbf{1}^+$ and $\mathbf{2}^+$ are shown in Figs. S14 and S15, where the overlays of the X-ray structures and that of the free ligand (DFT optimized geometry) are shown.

The molecular packing (see Figs. S12 and S13) consists of a complex network of hydrogen-bonds between the oxygens of H_2O molecules, the N atoms of the ligand and of the nitrate counterions (in the range 2.8–3.2 Å) and π- π stacking interactions (at ca. 3.8 Å) between the ligands (see Figs. S16 and S17).

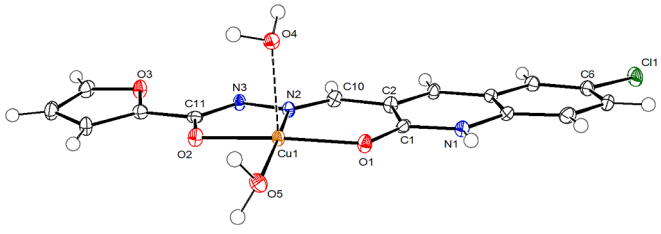

Fig. 2. Ortep view of one of the two independent cations (Mol A) in the unit cell of **2**(NO_3) (ellipsoid drawn at 50% probability).

Table 2
Selected Bond Lengths (Å) and Angles (deg) for the cation ($\mathbf{2}^+$, Mol A) together with the corresponding DFT calculated values.

	X-ray	Methanol[a]	Vacuum[a]
Cu1-O1	1.931(2)	1.981	1.931
Cu1-O2	1.942(2)	1.981	1.914
Cu1-O4	2.349(2)	2.395	2.326
Cu1-O5	1.960(2)	2.038	2.038
Cu1-N2	1.935(3)	1.972	1.938
Cl1-C6	1.745(3)	1.764	1.744
O1-C1	1.260(4)	1.258	1.262
O2-C11	1.288(4)	1.289	1.302
N2-N3	1.392(4)	1.372	1.359
N2-C10	1.288(4)	1.290	1.296
N1-C1	1.354(4)	1.360	1.369
N1-C9	1.384(4)	1.378	1.383
O1-Cu1-O2	172.28(9)	172.62	175.76
O1-Cu1-O4	92.89(9)	89.42	94.86
O2-Cu1-O4	94.09(9)	92.28	86.87
O1-Cu1-O5	91.98(9)	91.44	93.14
O2-Cu1-O5	92.69(9)	95.83	90.99
N2-Cu1-O5	169.9(1)	175.96	168.88
N2-Cu1-O4	98.7(1)	93.21	109.24
N3-N2-C10	117.1(3)	117.82	118.70
N2-N3-C11	108.6(2)	109.94	110.02

[a] Data calculated at B3LYP-GD3/6-311G(d,p) both in a vacuum and by considering the bulk solvent methanol.

3.2.3. *Solid state structure of 3: [(L2)Cu(NO_3)(CH_3OH)]·2CH_3OH*

Fig. 3 shows an ORTEP view of complex **3**, while a list of relevant bond lengths and angles is given in Table 3. The immediate coordination sphere of the Cu centre is defined by the O2, N2 and O3 atoms of the $\mathbf{L2}^-$ ligand (Scheme 1) and the O5 atom of the η^1-coordinated nitrate. The oxygen atom of a weakly interacting solvent molecule (CH_3OH, Cu1-O4 2.246(1) Å) completes a slightly distorted square pyramidal coordination, with the Cu atom ca. 0.4 Å above the plane defined by atoms O1, O2 and N2 (Table S22).

The bond lengths and angles are in the expected range and comparable to those found in related Cu-hydrazone complexes [46,49]. There are no significant differences in the geometrical parameters of complex **3** and those of **1**(NO_3) and **2**(NO_3) except for those involving the weakly bonded H_2O, CH_3OH and NO_3^- ion that, in the solid state, are strongly affected by the packing interactions. We also note that these molecules are those that are easily exchanged in solution.

As in the complexes previously discussed, upon coordination, the ligand is only slightly distorted making a dihedral angle between the planar dihydroquinoline and furan rings of ca. 4.6°.

The molecular packing is dictated by a network of strong hydrogen-bonds. The relevant atoms are the oxygen atoms of the two uncoordinated H_2O molecules (or the symmetry related ones) and the N1 and O2 atoms (O—N 2.77 Å, O—O 2.76 Å, respectively, Figs. S20–S22). We also note π- π stacking interactions (in the range 3.3–3.4 Å) between the planar quinoline and furan rings (Fig. S23). Moreover, there is a weak electrostatic interaction between the O6 atom of the coordinated nitrate

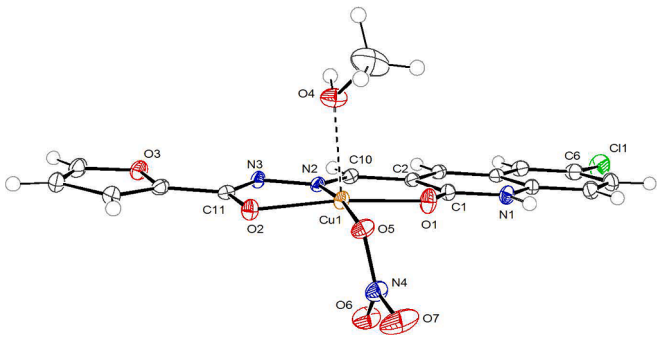

Fig. 3. Ortep view of complex **3** (ellipsoid drawn at 50% probability).

Table 3
Selected Bond Lengths (Å) and Angles (deg) for complex **3** together with the corresponding DFT calculated values.

	X-ray	Methanol[a]	Vacuum[a]
Cu1-O1	1.947(1)	1.981	2.044
Cu1-O2	1.970(1)	1.981	1.999
Cu1-O4	2.246(1)	2.439	2.286
Cu1-O5	1.970(1)	2.000	1.933
Cu1-N2	1.947(1)	1.975	1.980
Cl1-C6	1.741(2)	1.765	1.755
O1-C1	1.261(2)	1.257	1.243
O2-C11	1.290(2)	1.288	1.276
N2-N3	1.390(2)	1.373	1.355
N2-C10	1.286(2)	1.291	1.298
N1-C1	1.350(2)	1.360	1.369
N1-C9	1.379(2)	1.377	1.380
O1-Cu1-O2	169.51(5)	171.34	167.70
O1-Cu1-O4	98.72(5)	96.30	84.26
O2-Cu1-O4	89.79(5)	87.47	90.22
O1-Cu1-O5	90.76(5)	93.00	91.74
O2-Cu1-O5	95.28(5)	94.91	99.82
N2-Cu1-O5	172.91(5)	174.87	169.30
N2-Cu1-O4	95.16(5)	94.02	94.18
N2-Cu1-O1	92.15(5)	91.36	89.10
N2-Cu1-O2	80.91(5)	80.57	80.34
N3-N2-C10	117.0(1)	117.49	117.02
N2-N3-C11	109.5(1)	109.96	109.78
O6-N4-O5	118.0(1)	119.19	116.02
O7-N4-O5	118.7(1)	118.01	119.35
O7-N4-O6	123.4(1)	122.79	124.63

[a] Data calculated at B3LYP-GD3/6-311G(d,p) both in a vacuum and by considering the bulk solvent methanol.

and the Cu centre at 2.63 Å.

3.3. EPR data

The EPR spectra of the **1**(NO_3), **2**(NO_3) and **3** in frozen matrix (MeOH) at 140 K are reported in Figs. 4–6. The EPR spectra of the Cu(II) complexes were characterized by a quartet of lines at low-fields (the so-called parallel region) and a strong line at higher field (perpendicular region). The parallel region is the most informative: the position of the quartet (related to the g_z parameter) and the distance between the lines (the A_z parameter) give information concerning the copper coordination sphere. The g_z values (higher than g_x and g_y) are in agreement with Cu

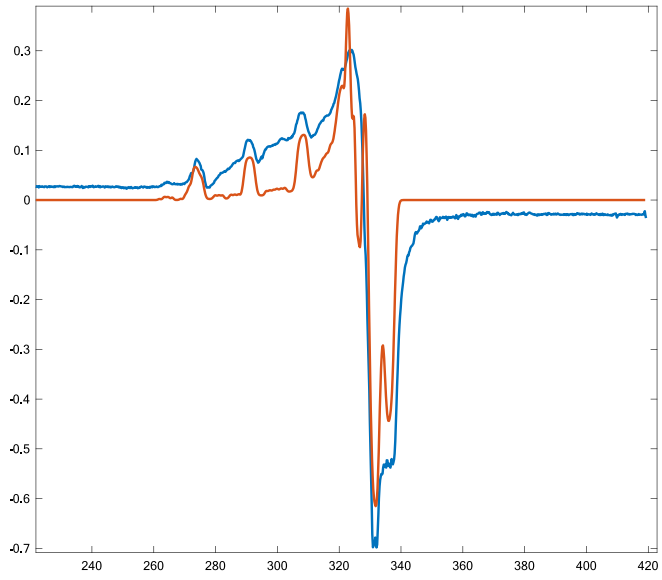

Fig. 4a. EPR spectrum of **1**(NO_3) (blue) and simulated (red). On the abscissa, the field values in mT.

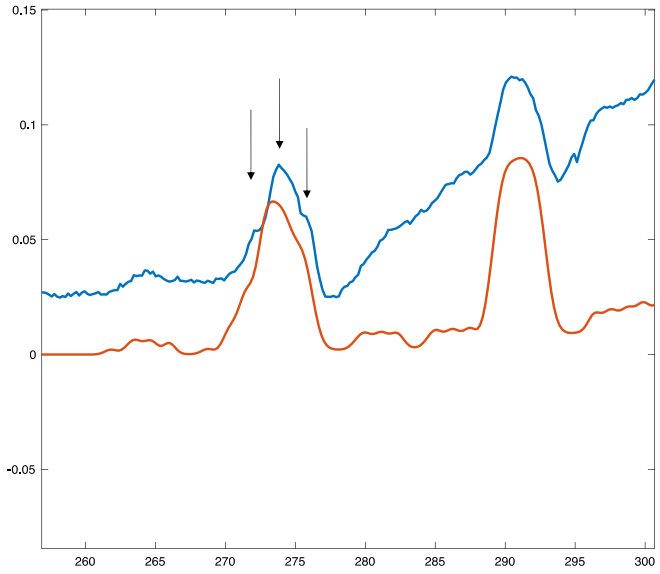

Fig. 4b. Parallel region of the EPR spectrum of **1**(NO_3) with highlighted hyperfine nitrogen structure.

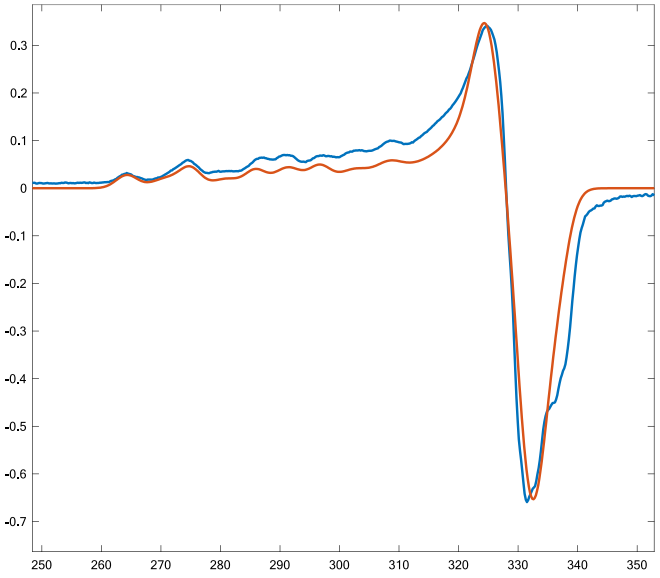

Fig. 5a. EPR spectrum of **2**(NO_3) (blue) and simulated (red). On the abscissa, the field values in mT.

(II) complexes in the fundamental state d_{x2-y2}. The spectrum of **1**(NO_3) (Fig. 4a) shows the presence of two further quartets, with significantly less intense lines, according to the data reported in Table 4. The different species can be originated by H_2O, MeOH or NO_3^- ion differently interacting with the copper atom. Species A1 shows a reduced g_z and an increased A_z with respect to species B1 and C1, which is indicative of an increased covalent bonding and/or a decreased complex charge with respect to B1 and C1 [64,65]. In addition, the main quartet lines of A1 exhibit "shoulders" (Fig. 4b) indicative of hyperfine splitting with a coordinated nitrogen, in agreement with the ONO coordination. B1 and C1 have higher g_z values, suggesting species with a higher positive charge.

The EPR spectrum of **2**(NO_3) also shows the presence of three species where, A2 reasonably similar to A1, is not the most abundant one (Fig. 5). B2 and C2 species, quite similar to each other, with the B2 the most abundant, show parameters quite different from A2, and also different from B1 and C1: a particularly low value of the hyperfine

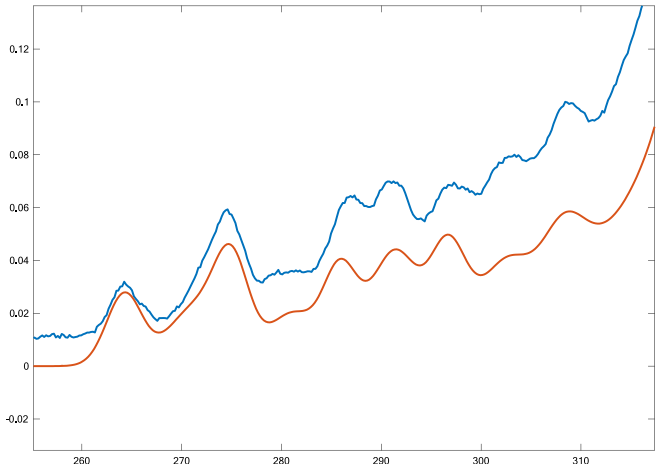

Fig. 5b. Parallel region of the EPR spectrum of **2**(NO_3).

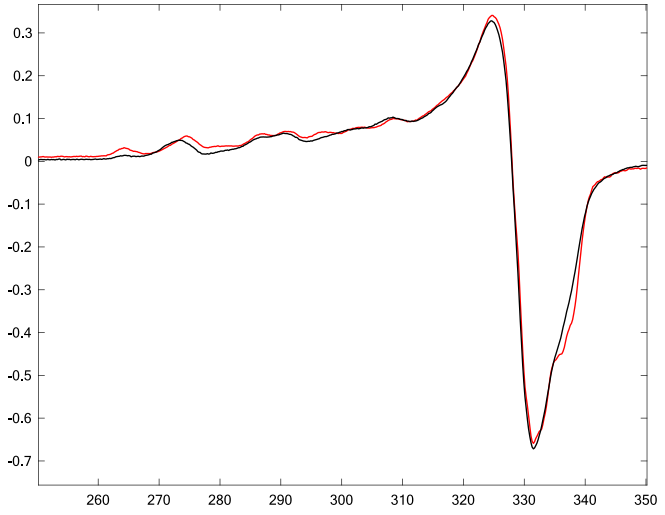

Fig. 6a. EPR spectrum of **3** (black) and of **2**(NO_3) (red). On the abscissa, the field values in mT.

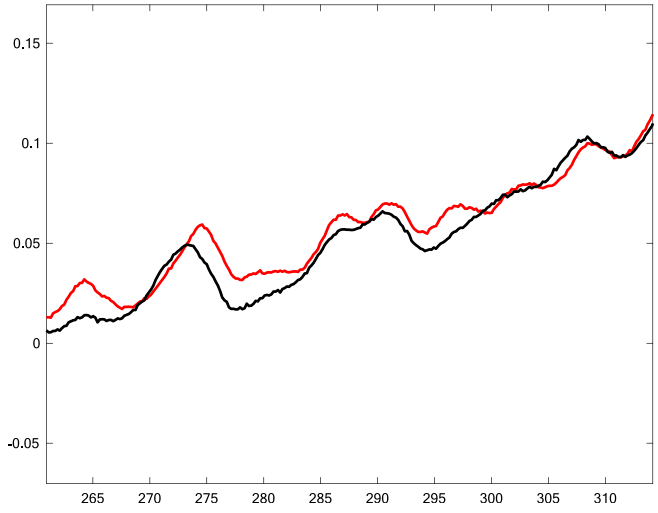

Fig. 6b. Parallel region of the EPR spectra of **3** (black) and **2**(NO_3) (red).

coupling, with a very high value of g_z, which are not fully consistent with an ONO coordination geometry around the copper. A possible explanation could be the formation of supramolecular dimeric aggregates, due to weak dispersive forces, resulting in spin-delocalization and reduction of the hyperfine coupling.

In Fig. 6 the EPR spectra of **2**(NO_3) and **3**, dissolved in methanol, are shown: the pattern of the species is very similar, with just minor differences, related to a slightly different ratio of species and/or different line widths. Calculated EPR data showed that the species guessed from the EPR spectra are ascribable to the occurrence of a complex dynamic in solution involving several configurations due to the coordinated water and/or methanol and/or the proximity of the NO_3^- anion to the metal complexes (see Table S24 and further details as Supplementary Materials). Moreover, consistent with the calculations, is the presence of **2**(NO_3) supramolecular dimeric aggregates (Fig. S8). This possibility was suggested by the relatively close intermolecular contacts between MolA and MolB in the asymmetric unit of **2**(NO_3) that may indicate that a dimeric supramolecular moiety in the solid may persist in solution, an assumption confirmed by the experimental and calculated spectra.

Due to the similarity of the EPR spectra for **2**(NO_3) and **3**, we can infer that also **3** shows the same tendency to aggregate in the conditions used to acquire the EPR spectra, whereas **1**(NO_3) seems less prone to do this.

3.4. Computational study of the solvent exchange on the complexes' inner coordination sphere

EPR spectra showed, on the timescale of the EPR experiment, the occurrence in frozen matrix (MeOH) of three main resonance patterns for both the complexes **1**(NO_3) and **2**(NO_3) (Table 4). It was guessed that these patterns could correspond to transient species characterized by different solvent molecules (water and/or methanol) coordinated to Cu^{II}, by different interactions/orientation of the negative counterion NO_3^-, and by the probable occurrence of a dimeric aggregate for **2**(NO_3), the latter conceivably due to the low temperature condition needed for EPR spectra. Thus, the calculation of the EPR parameters early discussed (see EPR data §3.3) was performed on several model systems to assess the hypotheses guessed from the experimental data. Due to the complex dynamic in solution caused by the occurrence of several configurations, we have set up some limiting species potentially present in solution, to picture the general trend of solvent exchanges occurring in the system. In this context, the EPR calculations were preceded by a preliminary investigation concerning the coordination thermodynamics of water and methanol in the complexes on the models considered. Incidentally, the standard Gibbs free energy variations (ΔG°) associated with the solvent replacement process (Table 5) were calculated by considering both the cationic species – where the NO_3^- has been assumed quite far from the metal complex – and neutral species where the nitrate ion is close to the first coordination sphere of the metal center, being these ones considered in order to evaluate the anion proximity effects.

The calculated ΔG values in Table 5 indicate that, for both complexes, the solvent exchange process occurs easily in slightly different ways. Indeed, exchange seems ergonically more unfavored for those models where is considered the NO_3^-. Nonetheless, the energies involved are quite low indicating that each of the solvent exchange processes could occur quite easily at room temperature and suggesting the occurrence of several species in frozen methanol matrix.

Finally, we also investigated the solvent exchange involving the DMSO to assess the probable chemical species occurring in the samples for any biological assays. In this context, we studied in detail the thermodynamics of the coordination chemistry of the exchange process involving DMSO, H_2O, and methanol towards **1**(NO_3) and **2**(NO_3) in water solution. The calculated coordination Gibbs free energies confirmed the higher coordination behavior of the DMSO than water and methanol towards the complexes. Nonetheless, the ΔG variations, ranging from about 20 to 30 kJ/mol, indicate that the replacement of the

Table 4
EPR data for **1**(NO_3) and **2**(NO_3).

	Species	g_x	g_y	g_z	A_x (MHz)	A_y (MHz)	A_z (MHz)	%
1(NO_3)	A1	2.060	2.105	2.275	30	30	534	80
	B1	2.090	2.095	2.320	50	50	480	10
	C1	2.100	2.110	2.355	50	50	540	10
2(NO_3)	A2	2.070	2.070	2.275	50	50	540	24
	B2	2.060	2.080	2.430	50	50	360	48
	C2	2.070	2.070	2.380	50	50	350	28

Table 5
Calculated standard Gibbs free energies values concerning the solvent exchange process at the copper centre. Data have been obtained by considering the methanol as bulk solvent by the SMD approach.

Solvent replacement reaction (methanol as bulk solvent)	ΔG (kJ/mol)
[1··2H_2O] $^+$ + MeOH<==> **[1·H_2O,MeOH]** $^+$ + H_2O	−4.98
[1·H_2O,MeOH] $^+$ + MeOH<==> **[1·2MeOH]** $^+$ + H_2O	3.22
[1··2H_2O] [NO_3] + MeOH<==> **[1·H_2O,MeOH] [NO_3]** + H_2O	14.94
[1·H_2O,MeOH] [NO_3] + MeOH<==> **[1·2MeOH] [NO_3]** + H_2O	−13.64
[2··2H_2O] $^+$ + MeOH<==> **[2·H_2O,MeOH]** $^+$ + H_2O	−1.93
[2·H_2O,MeOH] $^+$ + MeOH<==> **[2·2MeOH]** $^+$ + H_2O	−5.48
[2··2H_2O] [NO_3] + MeOH<==> **[2·H_2O,MeOH] [NO_3]** + H_2O	12.85
[2·H_2O,MeOH] [NO_3] + MeOH<==> **[2·2MeOH] [NO_3]** + H_2O	4.77

DMSO by the H_2O in water solution, should not be a difficult process (results are given in Table S25).

3.5. DNA binding studies

The binding modes of the copper complexes **1**(NO_3) and **2**(NO_3) were investigated through electronic absorption titrations in the presence of calf thymus (CT)-DNA. Due to solubility problems, it was not possible to perform this study with the free ligands. Usually, the binding of any compound to DNA through intercalation results in hypochromism with or without a small red or blue shift due to the strong stacking interaction between the planar aromatic chromophore and the DNA base pair [66,67].

Fig. 7 shows representative UV–VIS spectra of the copper complexes in the absence and in the presence of CT-DNA. Upon increasing the DNA concentration, the absorption bands of the complex **1**(NO_3) exhibited hypochromism of 28.7 % at 249 nm, 27.1 % at 359 nm, and 39.6 % at 393 nm, while those of complex **2**(NO_3) of 23.8 % at 260 nm, 29.2 % at 363 nm, 32.2 % at 396 nm, respectively, with blue shifts of 0–3 nm. The hypochromism suggests that the copper complexes bind to the DNA helix via intercalation. To find out the magnitude of the binding strength of the compounds with DNA, their intrinsic binding constants (K_b) were determined according to the following equation:

$$[DNA]/(\varepsilon_a - \varepsilon_f) = [DNA]/\{(\varepsilon_b - \varepsilon_f) + 1\ K_b(\varepsilon_b - \varepsilon_f)\}$$

where [DNA] is the concentration of DNA in base pairs, ε_a is the apparent absorption coefficient corresponding to A_{obs}/[compound]; ε_f is the extinction coefficient of the free compound and ε_b is the extinction coefficient of the compound when fully bound to DNA.

From the plot of [DNA]/(ε_a-ε_f) vs [DNA] (Fig. 8) the intrinsic constant K_b were calculated by the slope of the intercept. The K_b values were found to be 4.23(±0.01)·10^4 M^{-1} and 3.52(±0.07)·10^4 M^{-1}, for compounds **1**(NO_3) and **2**(NO_3), respectively. These values are in agreement with those reported for many NxOy-Cu(II)-coordinated systems [25,46,47,49,51,52,68].

3.6. Cytotoxicity studies

The in vitro antitumor activity of the new Cu(II) complexes **1**(NO_3) and **2**(NO_3) and of the uncoordinated ligands (**HL1** and **HL2**) has been

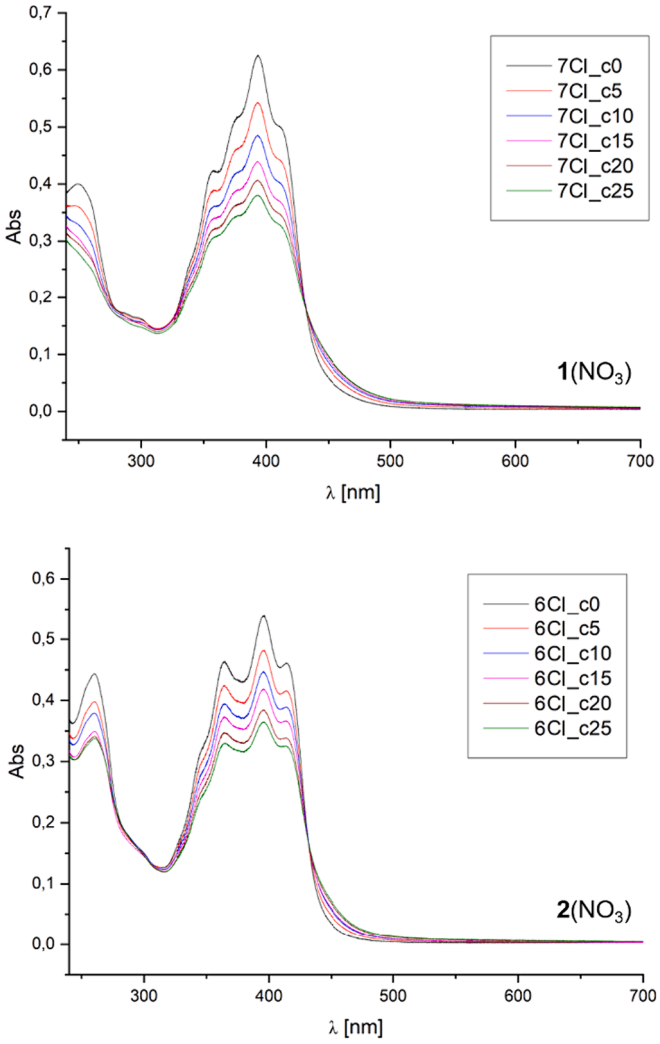

Fig. 7. Electronic spectra of copper complex **1**(NO_3) and **2**(NO_3) in tris-HCl buffer (pH = 8.2) upon addition of increasing concentrations of CT-DNA. [Compound] = 25 μM; [DNA] = 0–25 μM.

evaluated against some human cancer cell lines derived from solid tumors with different sensitivity to the reference metal-based chemotherapeutic cisplatin. The cytotoxicity parameters, expressed in terms of IC50 calculated from dose-survival curves obtained after 72 h exposure to the MTT test, are listed in Table 7. Cell lines representative of pancreatic (BxPC3 and PSN-1), cervical (A431), colon (HCT-15) and lung (H157) have been selected for the preliminary screening.

The cytotoxicity results showed that both copper complexes exhibited a noticeable antiproliferative activity, with IC50 values in the micromolar range against all tested cancer cell lines when compared to that of the ligands **HL1** and **HL2** that proved to be scarcely effective (the average IC50 values were over 25 μM).The cytotoxic profiles of **1**(NO_3)

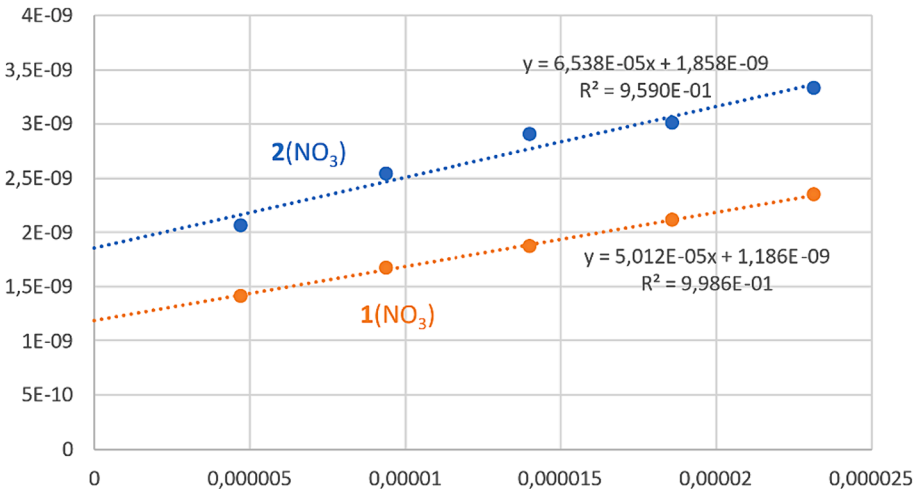

Fig. 8. Plots of [DNA]/(ε_a-ε_f) vs [DNA] of the complexes **1**(NO_3) and **2**(NO_3).

Table 7
Cytotoxicity studies.

IC50 (μM) ± S.D.					
Compounds	HCT-15	H157	BxPC3	PSN-1	A431
1(NO_3)	16.4 ± 3.5	5.4 ± 0.9	10.4 ± 2.5	3.9 ± 0.3	3.5 ± 0.2
HL1	> 25	17.5 ± 2.6	> 25	20.5 ± 3.1	> 25
2(NO_3)	14.5 ± 3.6	9.0 ± 0.5	11.8 ± 1.6	4.7 ± 0.8	2.3 ± 0.7
HL2	> 25	> 25	> 25	> 25	> 25
cisplatin	15.5 ± 3.8	6.2 ± 1.3	13.9 ± 5.9	13.5 ± 4.1	2.1 ± 0.9

Cells (3–8·10^3 ml^{-1}) were treated for 72 h with increasing concentrations of tested compounds dissolved in DMSO. Cytotoxicity was assessed by MTT test. IC_{50} values were calculated by four parameter logistic model ($P < 0.05$).

and **2**(NO_3) were on the average very similar, thus suggesting that the chlorine position in the coordinated ligands does not significantly influence the cytotoxic efficacy. Both copper complexes were more effective or at least as effective as cisplatin in inhibiting cancer cell growth. It is to be mentioned that both the complexes were markedly very effective against pancreatic PSN-1 cells showing IC50 values about 3-fold lower than those calculated for the reference drug. The data reported in Table 7 demonstrate that **1**(NO_3) and **2**(NO_3) showed a similar or slightly lower cytotoxic potential if compared to previously reported copper complexes containing 2-oxo-1,2-dihydrobenzo[*h*]quinoline-3-carbaldeyde bearing phenol groups as Y moieties in the hydrazones X-C(Z) = *N*-NH-C(=O)Y, [47] but higher with respect to other quinoline copper derivatives [46,47,49,51].

Considering that drug resistance represents a key determinant for the variable efficacy of anticancer therapy, the antiproliferative activity of the newly synthesized copper complexes was investigated on additional ovarian (A2780) and colon (LoVo) cancer cell lines whose sublines were suitably selected for the multidrug resistant phenotype (A2780 MDR) or the resistance to oxaliplatin (LoVo OXP). The cytotoxicity was evaluated by means of the MTT test after 72 h treatment with increasing concentrations of the test compounds. IC_{50} values, calculated from dose–survival curves, are shown in Table 8. Cross-resistance profiles were expressed in terms of the resistance factor, RF, which is defined as the ratio between the IC50 value for the resistant cells and that arising from the parent cells. Compared to human ovarian A2780 cells, A2780 MDR cells were about 16-fold more resistant to doxorubicin, a drug belonging to the MDR spectrum, whereas LoVo OXP cells were about 17-fold more resistant to oxaliplatin than parental cells. Here again, both **1**(NO_3) and **2**(NO_3) showed a similar pattern of activity, being both equally cytotoxic to sensitive and resistant cells, thus proving to be capable of overcoming the multidrug and oxaliplatin resistances.

Table 8
Cross-resistance profiles.

IC50 (mM) ± S.D.						
Compound	A2780	A2780 ADR	R.F.	LoVo	LoVoOxPt	R.F.
1(NO_3)	2.7 ± 0.4	3.4 ± 0.2	1.3	4.6 ± 0.6	4.2 ± 0.5	0.9
2(NO_3)	2.6 ± 0.6	3.7 ± 0.6	1.4	2.3 ± 0.4	2.1 ± 0.9	0.9
Doxorubicin	0.01 ± 0.005	0.16 ± 0.03	16.0	–	–	–
Oxaliplatin	–	–	–	3.1 ± 0.3	53.4 ± 0.8	17.1

S.D. = standard deviation. IC_{50} values were calculated by four parameter logistic model ($P < 0.05$). Cells (3-8·10^3·ml^{-1}) were treated for 72 h with increasing concentrations of tested compounds dissolved in DMSO. Cytotoxicity was assessed by MTT test. R.F. = IC_{50} (resistant subline)/IC_{50} (wild-type cells).

Though if it is not easy to compare the results reported in the literature due to the different cancer cell lines tested, we could observe that in the case of Cu(II) complexes bearing X = benzoquinoline, Z = H and Y = C_6H_5-OH moieties in the hydrazone X-C(Z) = *N*-N=C(-O)Y ligands, the IC_{50} values against A431 cell lines were comparable to those observed for the complexes **1**(NO_3) and **2**(NO_3) here reported, while in the case of the HCT-15 cell lines, **1**(NO_3) and **2**(NO_3) showed a lower efficacy, with IC_{50} values in all cases lower than 10 μM. [47]. On the contrary, in the case of the copper complexes bearing X = dihydroquinoline, Z = H and Y = o-C_6H_5-OH, the IC_{50} values were about 20–30 μM [46]. As for the influence of the furan group present as the Y moiety in **1**(NO_3) and **2**(NO_3), it was reported that for hydrazone Cu(II) complexes of the ligands Py-CH-N = NH-C(=O)-W, when W = pyridine, the compound was able to protect methionine from oxidation but histidine oxidation was promoted, while with W = furan, prevention of both methionine and histidine oxidation was observed [41]. In the case of hydrazone ruthenium complexes [69,70], the presence of a furan moiety has not significantly influenced the cytotoxicity even in the presence of phenyl, pyridine or thiophene groups. Finally, a comparison can be also done with the cytotoxic activity of complex reported in Ref. [71] bearing the 6-Cl-dihydroquinoline moiety as the ligand, which showed results similar to that of cisplatin against A549 and MCF7 cell lines.

4. Conclusions

The formation of three new Cu(II) complexes from two different

hydrazones depended on the crystallization conditions giving rise to complexes **1**(NO_3) and **2**(NO_3) where two H_2O molecules are coordinated, but in **3** a MeOH and a NO_3^- bonded to the copper centre. The formation of three species was also observed in the EPR spectra for **1**(NO_3) and **2**(NO_3) in frozen MeOH. A detailed computational study demonstrated that the solvent molecules can be easily exchanged in the Cu(II) coordination sphere, thus different species could be formed in the presence of excess water or MeOH. A good agreement was observed between the experimental EPR data and the calculated ones. As expected, the DMSO used to dissolve the complexes for the DNA binding and the cytotoxicity studies showed that DMSO can easily substitute both H_2O and MeOH in the coordination sphere, but can in turn be replaced by water in the cell culture medium. Thus, we could reasonably imagine that the $LCu(H_2O)_2$ species are the compounds interacting with DNA and the cells. Even if other cellular targets can be present for complexes **1**(NO_3) and **2**(NO_3), they showed DNA binding with intrinsic constant K_b of about 4×10^4 and exhibited a noticeable antiproliferative activity against a panel of human cancer cell lines together with the ability to overcome multidrug and oxaliplatin resistance.

To achieve further insight on the biological activity of this type of complexes, it is worthwhile to investigate the role of chlorine, or in general of a halogen atom in the structure for their possible involvement in halogen-bonding within the cellular environment which is rich in polar electrophilic and nucleophilic sites, thus stabilizing inter- and/or intramolecular interactions that can affect the compounds binding and molecular folding.

CRediT authorship contribution statement

Thangavel Thirunavukkarasu: Writing – original draft, Investigation. **Hazel A. Sparkes:** Writing – original draft, Investigation. **Valentina Gandin:** Writing – original draft, Investigation. **Cristina Marzano:** Writing – original draft, Investigation. **Roberta Bertani:** Writing – original draft, Supervision, Conceptualization. **Mirto Mozzon:** Writing – original draft, Investigation. **Anna Scettri:** Writing – original draft, Investigation. **Alberto Albinati:** Writing – original draft, Investigation, Data curation. **Francesco Demartin:** Writing – original draft, Investigation. **Girolamo Casella:** Writing – original draft, Investigation, Data curation. **Francesco Ferrante:** Writing – original draft, Investigation. **Alfonso Zoleo:** Writing – original draft, Investigation. **Paolo Sgarbossa:** Writing – original draft, Investigation, Conceptualization. **Karuppannan Natarajan:** Writing – original draft, Supervision, Conceptualization.

Declaration of competing interest

The authors declare that they have no known competing financial interests or personal relationships that could have appeared to influence the work reported in this paper.

Data availability

The data presented in this study are available on reasonable request from the corresponding author.

Acknowledgement

The authors acknowledge the support of the research by the Department of Industrial Engineering.

Appendix A. Supplementary data

Supplementary data to this article can be found online at https://doi.org/10.1016/j.ica.2024.122022.

References

[1] E. Giorgi, F. Binacchi, C. Marotta, D. Cirri, C. Gabbiani, A. Pratesi, Molecules 28 (2023) 273, https://doi.org/10.3390/molecules28010273.
[2] R. Paprocka, M. Wiese-Szadkowska, S. Janciauskiene, T. Komalski, M. Kulik, A. Helmin-Basa, Coord. Chem. Rev. 452 (2022) 214307, https://doi.org/10.1016/j.ccr.2021.214307.
[3] T. Lazarevic, A. Rilak, Z.D. Bugarcic, Eur. J. Med. Chem. 142 (2017) 8, https://doi.org/10.1016/j.ejmech.2017.04.007.
[4] T.C. Johnstone, K. Suntharalingam, S.L. Lippard, Chem. Rev. 116 (2016) 3436, https://doi.org/10.1021/acs.chemrev.5b00597.
[5] A. Khoury, E. Elias, S. Mehanna, W. Shebaby, K.M. Deo, N. Mansour, C. Khalil, K. Sayyed, J.A. Sakoff, J. Gilbert, C.F. Daher, C.P. Gordon, R.I. Taleb, J.R. Aldrich-Wright, J. Med. Chem. 65 (2022) 16481, https://doi.org/10.1021/acs.jmedchem.2c01310.
[6] K.M. Deo, D.L. Ang, B. McGhie, A. Rajamanickam, A. Dhiman, A. Khoury, J. Holland, A. Bjelosevic, B. Pages, C. Gordon, J.R. Aldrich-Wright, Coord. Chem. Rev. 375 (2018) 148, https://doi.org/10.1016/j.ccr.2017.11.014.
[7] L. Bai, C. Gao, Q. Liu, C. Yu, Z. Zhang, L. Cai, B. Yang, Y. Qian, J. Yang, X. Liao, Eur. J. Med. Chem. 140 (2017) 349, https://doi.org/10.1016/j.ejmech.2017.09.034.
[8] G. Feng, X. Zhou, J. Chen, D. Li, L. Chen, Front. Oncol. 12 (2023) 1012093, https://doi.org/10.2289/fonc.2022.1012093.
[9] T. Huo, R.F. Barth, W. Yang, R.J. Nakkula, R. Koynova, B. Tenchov, A. R. Chaudhury, L. Agius, T. Boulikas, H. Elleaume, R.J. Lee, PLOS ONE 7 (2012) e48752.
[10] B.P. Esposito, R. Najjar, Coord. Chem. Rev. 232 (2002) 137, https://doi.org/10.1016/S0010-8545(02)00049-8.
[11] A. Bergamo, P.J. Dyson, G. Sava, Coord. Chem. Rev. 360 (2018) 17, https://doi.org/10.1016/j.ccr.2018.01.009.
[12] D.P. Gately, S.B. Howell, Brit. J. Cancer 67 (1993) 1171, https://doi.org/10.1038/bjc.1993.221.
[13] S. Ishida, J. Lee, D.J. Thiele, I. Herskowitz, Proc. Nat. Acad. Sci. USA 99 (2002) 14298, https://doi.org/10.1073/pnas.162491399.
[14] R.A. Alderden, M.D. Hall, T.W. Hambley, J. Chem. Edu. 83 (2006) 728, https://doi.org/10.1021/ED083P728.
[15] C. Santini, M. Pellei, V. Gandin, M. Porchia, F. Tisato, C. Marzano, Chem. Rev. 114 (2014) 815, https://doi.org/10.1021/cr400135x.
[16] S. Tardito, O. Bussolati, F. Gaccioli, R. Gatti, S. Guizzardi, J. Uggeri, L. Marchiò, M. Lanfranchi, R. Franchi-Gazzola, Histochem. Cell. Biol. 126 (2006) 473, https://doi.org/10.1007/s00418-006-0183-4.
[17] S. Dhar, D. Senapati, P.K. Das, P. Chattopadhyay, M. Nethaji, A.R. Chakravarty, J. Am. Chem. Soc. 125 (2003) 12118, https://doi.org/10.1021/ja036681q.
[18] S.Y. Tsang, S.C. Tam, I. Bremner, M.J. Burkitt, Biochem. J. 317 (1996) 13, https://doi.org/10.1042/bj3170013.
[19] E. Bencini, A. Berni, C. Bianchi, B. Giorgi, B. Valtancoli, D.K. Chand, H. J. Schneider, Dalton Trans. (2003) 793, https://doi.org/10.1039/b211001f.
[20] D.K. Chand, H.J. Schneider, A. Bencini, A. Bianchi, C. Giorgi, S. Ciattini, B. Valtancoli, Chem. Eur. J. 6 (2000) 4001, https://doi.org/10.1002/1521-3765(20001103)6:21%3C4001::aid-chem4001%3E3.3.co;2-i.
[21] E.L. Hegg, J.N. Burstyn, Coord. Chem. Rev. 173 (1998) 133, https://doi.org/10.1016/S0010-8545(98)00157-X.
[22] J. Easmon, G. Purstinger, G. Heinisch, T. Roth, H.H. Fiebig, W. Holzer, W. Jager, M. Jenny, J. Hofmann, J. Med. Chem. 44 (2001) 2164, https://doi.org/10.1021/jm000979z.
[23] F. Liang, C. Wu, H. Lin, T. Li, D. Gao, Z. Li, J. Wei, C. Zheng, M. Sun, Bioorg. Med. Chem. Lett. 13 (2003) 2469, https://doi.org/10.1016/S0960-894X(03)00489-X.
[24] M.F. Primik, S. Goschl, M.A. Jakupec, A. Roller, B.K. Keppler, V.B. Arion, Inorg. Chem. 49 (2011) 11084, https://doi.org/10.1021/ic101633z.
[25] V. Rajendiran, K. Karthik, M. Palaniandavar, H. Stoeckli-Evans, V.S. Periasamy, M. A. Akbarsha, B.S. Srinag, H. Krishnamurthy, Inorg. Chem. 46 (2007) 8208, https://doi.org/10.1021/ic700755p.
[26] S. Dhar, P.A. Reddy, M. Nethaji, S. Mahadevan, M.K. Saha, A.R. Chakravarty, Inorg. Chem. 41 (2002) 3469, https://doi.org/10.1021/ic0201396.
[27] S.S. Bhat, A.A. Kumbhar, H. Heptullah, A.A. Khan, V.V. Gobre, S.P. Gejji, V. G. Puranik, Inorg. Chem. 50 (2011) 545, https://doi.org/10.1021/ic101534n.
[28] J.P. Rada, J. Forté, G. Gontard, C.M. Bachelet, N.A. Rey, M. Salmain, V. Corcé, J. Biol. Inorg. Chem. 6 (2021) 675, https://doi.org/10.1007/s00775-021-01885-5.
[29] M. Sutradhar, E.C.B.A. Alegria, T.R. Barman, M.F.C. Guedes da Silva, C.M. Liu, A.J. L. Pombeiro, Front. Chem. 8 (2020), https://doi.org/10.3389/fchem.2020.00157 article 157.
[30] P.F. Lee, C.T. Yang, D. Fan, J.J. Vittal, J.D. Ranford, Polyhedron 22 (2003) 2781, https://doi.org/10.1016/S0277-5387(03)00402-9.
[31] M.C. Vineetha, M. Sithambaresan, Y.S. Nair, M.R.P. Kurup, Inorg. Chim. Acta 491 (2019) 93, https://doi.org/10.1016/j.ica.2019.03.040.
[32] M. Cindric, A. Bjelopetrovic, G. Pavlovic, V. Damjanovic, J. Lovric, D. Matkovic-Calogovic, V. Vrdoljak, New J. Chem. 41 (2017) 2425, https://doi.org/10.1039/c6nj03827a.
[33] M. Sutradhar, R. Rajeshwari, T.R. Barman, A.R. Fernandes, F. Paradinha, C. Roma-Rodrigues, M.F.C. Guedes da Silva, A.J.L. Pombeiro, J. Inorg. Biochem. 175 (2017) 267, https://doi.org/10.1016/j.inorgbio.2017.07.034.
[34] M. Sutradhar, E.C.B.A. Alegria, M.F.C. Guedes da Silva, L.M.D.R.S. Martins, A.J. L. Pombeiro, Molecules 21 (2016), https://doi.org/10.3390/molecules21040425 article 425.
[35] M.F. Iskander, T.E. Khalil, R. Werner, W. Haase, I. Svoboda, H. Fuess, Polyhedron 19 (2000) 949, https://doi.org/10.1016/S0277-5387(00)00340-5.

[36] K.K. Kim, T.S. Lange, R.K. Singh, L. Brard, BMC Cancer 10 (2010) article 72. http://biomedcentral.com/1471-2407/10/72.
[37] M.F. Iskander, T.E. Khalil, W. Haase, R. Werner, I. Svoboda, H. Fuess, Polyhedron 20 (2001) 2787, https://doi.org/10.1016/S0277-5387(01)00872-5.
[38] L. Pan, C.F. Wang, K. Yan, K. Zhao, G. Sheng, H. Zhu, X. Zhao, D. Qu, F. Niu, Z. You, J. Inorg. Biochem. 159 (2016) 22, https://doi.org/10.1016/j.jinorgbio.2016.02.017.
[39] S.R. Sheeja, N.Z. Mangalam, M. Sithambaresan, M.R.P. Kurup, S. Kaya, G. Serdaroglu, J. Molec. Struct. 1245 (2021) 131001, https://doi.org/10.1016/j.jmolstruc.2021.131001.
[40] R. Vafazadeh, Z. Moghadas, A.C. Willis, J. Coord. Chem. 68 (2015) 4255, https://doi.org/10.1080/00958972.2015.1096349.
[41] D.S. Cukierman, N. Bodnar, B.N. Evangelista, L. Nagy, C. Kallay, N.A. Rey, J. Biol. Inorg. Chem. 24 (2019) 1231, https://doi.org/10.1007/s00775-019-01700-2.
[42] M.M. Fousiamol, M. Sithambaresan, K.K. Damodaran, M.R.P. Kurup, Inorg. Chim. Acta 501 (2020) 119301, https://doi.org/10.1016/j.ica.2019.119301.
[43] Y. Gou, J. Li, B. Fan, B. Xu, M. Zhou, F. Yang, Eur. J. Med. Chem. 134 (2017) 207, https://doi.org/10.1016/j.ejmech.2017.04.026.
[44] H. Hosseini-Monfared, H. Falakian, R. Bikas, P. Mayer, Inorg. Chim. Acta 394 (2013) 526, https://doi.org/10.1016/j.ica.2012.08.022.
[45] Z.C. Liu, B.D. Wang, Z.Y. Yang, Y. Li, D.D. Qin, T.R. Li, Eur. J. Med. Chem. 44 (2009) 4477, https://doi.org/10.1016/j.eimech.2009.06.009.
[46] D.S. Raja, N.S.P. Bhuvanesh, K. Natarajan, Inorg. Chim. Acta 385 (2012) 81, https://doi.org/10.1016/j.ica.2011.12.038.
[47] E. Ramachandran, V. Gandin, R. Bertani, P. Sgarbossa, K. Natarajan, N.S. P. Bhuvanesh, A. Venzo, A. Zoleo, A. Glisenti, A. Dolmella, A. Albinati, C. Marzano, J. Inorg. Biochem. 182 (2018) 18, https://doi.org/10.1016/j.inorgbio.2018.01.016.
[48] G.S. Hegde, S.S. Bhat, S.P. Netalkar, P.L. Hegde, A. Kotian, R.J. Butcher, V. K. Revankar, Inorg. Chim. Acta 522 (2021) 120352, https://doi.org/10.1016/j.ica.2021.120352.
[49] D.S. Raja, N.S.P. Bhuvanesh, K. Natarajan, J. Biol. Inorg. Chem. 17 (2012) 223, https://doi.org/10.1007/s00775-011-0844-1.
[50] D.S. Raja, E. Ramachandran, N.S.P. Bhuvanesh, K. Natarajan, Eur. J. Med. Chem. 64 (2013) 148, https://doi.org/10.1016/j.ejmech.2013.03.040.
[51] D.S. Raja, N.S.P. Bhuvanesh, K. Natarajan, Eur. J. Med. Chem. 47 (2012) 73, https://doi.org/10.1016/j.ejmech.2011.10.024.
[52] T. Thirunavukkarasu, H.A. Sparkes, C. Balachandran, S. Awale, K. Natarajan, V. G. Gnanasoundari, J. Photochem, B. Photobiol, Biology 181 (2018) 59, https://doi.org/10.1016/j.jphotobiol.2018.02.013.
[53] X.P. Ye, T.F. Zhu, W.N. Wu, T.L. Ma, J. Xu, Z.P. Zhang, Y. Wang, L. Jia, Inorg. Chem. Commun. 47 (2014) 60, https://doi.org/10.1016/j.inoche.2014.07.022.
[54] A. Carvalho, B.M. Barbosa, J.S. Flores, P. do Carmo Goncalves, R. Diniz, Y. Cordeiro, C.O. Fernandez, D.S. Cukierman, N.A. Rey, J. Inorg. Biochem. 238 (2023) 112033, https://doi.org/10.1016/j.jinorgbio.2022.112033.
[55] A. Bax, S. Subramanian, J. Magn. Reson. 67 (1986) 565, https://doi.org/10.1016/0022-2364(86)90395-1.
[56] A. Bax, M.F. Summers, J. Am. Chem. Soc. 108 (1986) 2093, https://doi.org/10.1021/ja00268a061.
[57] G. Otting, K. Wuthrich, J. Magn. Reson. 76 (1988) 569, https://doi.org/10.1016/0022-2364(88)90361-7.
[58] M.J. Frisch, G.W. Trucks, H.B. Schlegel, G.E. Scuseria, M.A. Robb, J.R. Cheeseman, J.R.; G. Scalmani, V. Barone, G.A. Petersson, H. Nakatsuji, X. Li, M. Caricato, A.V. Marenich, J. Bloino, B.G. Janesko, R. Gomperts, B. Mennucci, H.P. Hratchian, J.V. Ortiz, A.F. Izmaylov, J.L. Sonnenberg, J. Williams, F. Ding, F. Lipparini, F. Egidi, J. Goings, B. Peng, A. Petrone, T. Henderson, D. Ranasinghe, V.G. Zakrzewski, J. Gao, N. Rega, G. Zheng, W. Liang, M. Hada, M. Ehara, K. Toyota, R. Fukuda, J. Hasegawa, M. Ishida, T. Nakajima, Y. Honda, O. Kitao, H. Nakai, T. Vreven, K. Throssell, J.A. Montgomery Jr., J.E. Peralta, F. Ogliaro, M.J. Bearpark, J.J. Heyd, E.N. Brothers, K.N. Kudin, V.N. Staroverov, T.A. Keith, R. Kobayashi, J. Normand, K. Raghavachari, A.P. Rendell, J.C. Burant, S.S. Iyengar, J. Tomasi, M. Cossi, J.M. Millam, M. Klene, C. Adamo, R. Cammi, J.W. Ochterski, R.L. Martin, K. Morokuma, O. Farkas, J.B. Foresman, D.J. Fox, Gaussian 16 Revision B (2016), 01.
[59] S. Grimme, J. Antony, S. Ehrlich, H. Krieg, J. Chem. Phys. 132 (2010) 154104, https://doi.org/10.1063/1.3382344.
[60] A.V. Marenich, C.J. Cramer, D.G. Truhlar, J. Phys. Chem. B 113 (2009) 6378, https://doi.org/10.1021/jp810292n.
[61] V. Gandin, C. Ceresa, G. Esposito, S. Indracolo, M. Porchia, F. Tisato, C. Santini, M. Pellei, C. Marzano, Scientific Rep. 7 (2017) 13936, https://doi.org/10.1038/s41598-017-13698-1.
[62] M.N. Chaur, D. Collado, J.M. Lehn, Chem. Eur. J. 17 (2011) 248, https://doi.org/10.1002/chem.201002308.
[63] D.P. Fairlie, T.C. Woon, W.A. Wickramasinghe, A.C. Willis, Inorg. Chem. 33 (1994) 6425, https://doi.org/10.1021/ic00104a067.
[64] F. Dimiza, S. Fountoulaki, A.N. Papadopoulos, C.A. Kontogiorgis, V. Tangoulis, V. Psycharis, A. Terzis, D.P. Kessissoglou, G. Psomas, Dalton Trans. 40 (2011) 8555, https://doi.org/10.1039/c1dt10714c.
[65] M.C.R. Symons, D.X. West, J.G. Wilkinson, J. Chem. Soc. Dalton Trans. (1975) 1696, https://doi.org/10.1039/DT9750001696.
[66] F.A. Tanious, D. Ding, D.A. Patrick, C. Bailly, R.R. Tidwell, W.D. Wilson, Biochemistry 39 (2000) 12091, https://doi.org/10.1021/bi001236i.
[67] L. Jie, Z. Hao, C. Caihong, D. Hong, L. Tongbu, J. Liangnian, Dalton Trans. (2003) 114, https://doi.org/10.1039/b206079p.
[68] T. Thirunavukkarasu, H.A. Sparkes, K. Natarajan, V.G. Gnanasoundari, Appl. Organomet. Chem. (2018) e4403.
[69] M.E. Jung, B.T. Chamberlain, C.L. Ho, E.J. Gillespie, K.A. Bradley, A.C.S. Med, Chem. Lett. 5 (2014) 363, https://doi.org/10.1021/ml400486k.
[70] M. Alagesan, P. Sathyadevi, P. Krishnamoorthy, N.S.P. Bhuvanesh, N. Dharmaraj, Dalton Trans. 43 (2014) 15829, https://doi.org/10.1039/c4dt01032a.
[71] T. Thirunavukkarasu, H. Puschmann, H.A. Sparkes, K. Natarajan, V.G. Gnanasoundari, Applied Organomet. Chem. (2017) e4111. doi:10.022/aoc.4111.